

# REPORT DOCUMENTATION PAGE

*Form Approved*  
*OMB No. 0704-0188*

Public reporting burden for this collection of information is estimated to average 1 hour per response, including the time for reviewing instructions, searching existing data sources, gathering and maintaining the data needed, and completing and reviewing this collection of information. Send comments regarding this burden estimate or any other aspect of this collection of information, including suggestions for reducing this burden to Department of Defense, Washington Headquarters Services, Directorate for Information Operations and Reports (0704-0188), 1215 Jefferson Davis Highway, Suite 1204, Arlington, VA 22202-4302. Respondents should be aware that notwithstanding any other provision of law, no person shall be subject to any penalty for failing to comply with a collection of information if it does not display a currently valid OMB control number. **PLEASE DO NOT RETURN YOUR FORM TO THE ABOVE ADDRESS.**

|   |                    |   |                                   |   |  |
|---|--------------------|---|-----------------------------------|---|--|
| <b>1. REPORT DATE (DD-MM-YYYY)</b><br>20-10-2005  |                    | <b>2. REPORT TYPE</b><br>Conference Paper |                                   | <b>3. DATES COVERED (From - To)</b>   |  |
| <b>4. TITLE AND SUBTITLE</b><br><br>Ablation of Liquids for Laser Propulsion with TEA CO <sub>2</sub> Laser (POSTPRINT)   |                    |   |                                   | <b>5a. CONTRACT NUMBER</b>  |  |
|   |                    |   |                                   | <b>5b. GRANT NUMBER</b>   |  |
|   |                    |   |                                   | <b>5c. PROGRAM ELEMENT NUMBER</b>   |  |
| <b>6. AUTHOR(S)</b><br>John Sinko, Lisa Kodgis, Simon Porter, Enrique Sterling, Jun Lin and Andrew V. Pakhomov<br>(Dept of Physics, UA Huntsville); C. William Larson and Franklin B. Mead, Jr.<br>(AFRL/PRSP)  |                    |   |                                   | <b>5d. PROJECT NUMBER</b><br>4847   |  |
|   |                    |   |                                   | <b>5e. TASK NUMBER</b><br>0159  |  |
|   |                    |   |                                   | <b>5f. WORK UNIT NUMBER</b>   |  |
| <b>7. PERFORMING ORGANIZATION NAME(S) AND ADDRESS(ES)</b><br><br>Air Force Research Laboratory (AFMC)<br>AFRL/PRSP<br>10 E. Saturn Blvd.<br>Edwards AFB CA 93524-7680   |                    |   |                                   | <b>8. PERFORMING ORGANIZATION REPORT NUMBER</b><br><br>AFRL-PR-ED-TP-2005-396 |  |
| <b>9. SPONSORING / MONITORING AGENCY NAME(S) AND ADDRESS(ES)</b><br><br>Air Force Research Laboratory (AFMC)<br>AFRL/PRS<br>5 Pollux Drive<br>Edwards AFB CA 93524-70448  |                    |   |                                   | <b>10. SPONSOR/MONITOR'S ACRONYM(S)</b>                                       |  |
|   |                    |   |                                   | <b>11. SPONSOR/MONITOR'S NUMBER(S)</b><br>AFRL-PR-ED-TP-2005-396              |  |
| <b>12. DISTRIBUTION / AVAILABILITY STATEMENT</b><br><br>Approved for public release; distribution unlimited   |                    |   |                                   |   |  |
| <b>13. SUPPLEMENTARY NOTES</b><br>Presented at the 4 <sup>th</sup> International Symposium on Beamed Energy Propulsion, Nara, Japan, 11-14 Nov 2005.  |                    |   |                                   |   |  |
| <b>14. ABSTRACT</b><br>Time-resolved force sensing and intensified charge-coupled device (ICCD) imaging techniques were applied to the study of the force generation mechanism for laser ablation of liquids. A Transversely Excited at Atmospheric pressure (TEA) CO <sub>2</sub> laser operated at 10.6 μm, 300 ns pulse width, and 9 J pulse energy was used to ablate liquids contained in various aluminum and glass vessels. Net imparted impulse and coupling coefficient were derived from the force sensor data and relevant results will be presented for various container designs and liquids used. ICCD imaging was used in conjunction with the dynamic force techniques to examine dependencies on absorption depth, irradiance, surface curvature, and container geometry. ICCD imaging was also used to determine whether surface or volume absorption should be preferable for laser propulsion using liquid propellants. Finally, ballistic experiments were conducted in order to verify the dynamic force data and lend additional evidence as to the predominant methods of force generation. |                    |   |                                   |   |  |
| <b>15. SUBJECT TERMS</b>  |                    |   |                                   |   |  |
| <b>16. SECURITY CLASSIFICATION OF:</b>  |                    |   | <b>17. LIMITATION OF ABSTRACT</b> | <b>18. NUMBER OF PAGES</b>  | <b>19a. NAME OF RESPONSIBLE PERSON</b>                                       |
| <b>a. REPORT</b>  | <b>b. ABSTRACT</b> | <b>c. THIS PAGE</b>                       |                                   |   | Dr. Franklin B. Mead, Jr.  |
| Unclassified  | Unclassified       | Unclassified                              | A                                 | 12  | <b>19b. TELEPHONE NUMBER</b><br><i>(include area code)</i><br>(661) 275-5929 |

# Ablation of Liquids for Laser Propulsion with TEA CO<sub>2</sub> Laser

John Sinko, Lisa Kodgis, Simon Porter, Enrique Sterling, Jun Lin,  
and Andrew V. Pakhomov

*Department of Physics, The University of Alabama in Huntsville, Huntsville, AL 35899, USA*

C. William Larson and Franklin B. Mead, Jr.

*Propulsion Directorate, Air Force Research Laboratory, Edwards AFB, CA 93524-7680, USA*

**Abstract.** Time-resolved force sensing and intensified charge-coupled device (ICCD) imaging techniques were applied to the study of the force generation mechanism for laser ablation of liquids. A Transversely Excited at Atmospheric pressure (TEA) CO<sub>2</sub> laser operated at 10.6  $\mu\text{m}$ , 300 ns pulse width, and 9 J pulse energy was used to ablate liquids contained in various aluminum and glass vessels. Net imparted impulse and coupling coefficient were derived from the force sensor data and relevant results will be presented for various container designs and liquids used. ICCD imaging was used in conjunction with the dynamic force techniques to examine dependencies on absorption depth, irradiance, surface curvature, and container geometry. ICCD imaging was also used to determine whether surface or volume absorption should be preferable for laser propulsion using liquid propellants. Finally, ballistic experiments were conducted in order to verify the dynamic force data and lend additional evidence as to the predominant methods of force generation.

## INTRODUCTION

Interest has arisen recently in taking advantage of the high coupling coefficient ( $C_m$ ) in the laser ablation of liquids for propulsion, for instance as indicated by experiments by Prof. Takashi Yabe in which various craft were propelled via the ablation of water. In these experiments,  $C_m$  up to 350 dyne/W was observed [1,2].

The interaction of a laser with liquid is a somewhat complex process described at some length by Kim and Grigoropoulos [3]. As the laser pulse imparts energy to the liquid, if the pulse length is short compared to the characteristic time for thermal diffusion to take place, the process will be acoustically dominated. For longer pulses in excess of this regime, the process becomes thermal. In either case, at sufficient irradiance there is plasma formation, typically lasting up to several  $\mu\text{s}$  in air. Vaporization of the liquid surface is known to proceed up to several 10's of  $\mu\text{s}$  after the laser pulse. These processes are followed by the formation of a cavity or depression at the liquid surface (for surface absorption) or by bubble nucleation and/or

boiling within the liquid itself (for volume absorption). The deposited energy can also drive hydrodynamic effects like shock waves. If a surface cavity is formed, the ablated material forms a high-pressure region extending from the cavity into the ambient atmosphere. Depending on the distance scales involved and the energy deposited, subsequent behavior can include collapse of the cavity, bulk liquid splashing corona, ejected droplets, *etc.* For the purposes of this discussion, the term 'ablation' will describe any process of mass removal from the surface of interest.

Sterling *et al.* recently applied a piezoelectric force measurement technique developed by the Laser Propulsion Group (LPG) of UAH to liquid ablation [4,5]. In this study, a Lumonics TEA CO<sub>2</sub> laser was used to ablate water doped with varying concentrations of an absorbent material (*NaBF<sub>4</sub>*) in order to determine the effect upon the coupling coefficient. No significant change was observed under variation of the absorbent concentration. Since water absorbs very efficiently at 10.6 μm as shown in Table 1, we expect the ablation process for water to be dominated by surface vaporization.

Preliminary surface tension experiments with droplets of aqueous saturated solutions of detergent and *NaCl* on a flat surface indicated that altering the surface curvature of the liquid could significantly increase  $C_m$ . This led to an interest in whether other parameters involved might exhibit similar dependencies. The shape of the container, the shape of the liquid surface, and the absorption coefficient of the liquid were then investigated to determine whether variation of these parameters could increase  $C_m$ . ICCD imaging was performed to examine the various temporal regimes of liquid ablation (*e.g.* plasma formation, vaporization, splashing) in order to compare the results with dynamic force data. Finally, ballistics measurements were conducted in order to confirm the dynamic force results.

## EXPERIMENTAL SETUP

Single pulses of laser energy were delivered to the target by a Lumonics TEA CO<sub>2</sub> laser operating at 10.6 μm with a maximum beam power of approximately 10 J. The temporal profile consists of a 300 ns pulse with a 3 μs oscillatory ultraviolet N<sub>2</sub> tail. The energy of the laser beam was attenuated to 3.6 J, 1.2 J, and 0.4 J for various experiments by passing it through a series of PTFE (Teflon<sup>®</sup>) sheets with experimentally determined absorption properties. Laser power was measured with a standard laser power meter (Melles-Griot 13PEM001) after being directed to the test area with 2 planar gold mirrors. The laser light was focused using a ZnSe lens with 12" focal length.

Cylindrical and conical quartz glass containers, each capable of holding approximately 100 μl of liquid, were used in order to facilitate optical ICCD imaging of the cavity below the liquid surface. Each container had an inner diameter of approximately 6 mm at the rim and weighed approximately 1.6 g.

Several liquids with a wide range of absorption coefficients (Table 1) were chosen in order to gain an understanding of the dependence of the ablative process on absorption; *i.e.*, whether surface or volume absorption would be preferable for thrust generation. Hexane was chosen as a suitable candidate for volume interaction due to its negligible absorption at 10.6 μm. Ethanol was chosen as a probable intermediate

absorber; however, its behavior in experiments leads us to classify it as a surface absorber. Data was also collected for water and an aqueous solution of 70% isopropanol, all of which were observed to behave as surface absorbers. The approximate absorption coefficients for the various liquids, as determined from the NIST Quantitative IR Spectra Database for 10.6  $\mu\text{m}$ , are shown in Table 1 [6, 7].

**TABLE 1. Liquid Absorption Coefficients [6, 7].**

| Liquid   | Hexane     | Ethanol | Isopropanol | Water |
|--|------------|---------|-------------|-------|
| $\kappa$ ( $\text{cm}^{-1}$ ) for 10.6 $\mu\text{m}$ | negligible | 20      | 70          | 3000  |
| Absorption depth, $\mu\text{m}$                      | large      | 574     | 149         | 3     |

Impulse measurements were performed with piezoelectric force sensors (PCB-209C01 and PCB-200B02) characterized by  $\approx 5$   $\mu\text{s}$  rise time and better than  $10^{-3}$  N resolution. The sensors were connected through a signal conditioner (PCB-482B11) to a digital oscilloscope (Tektronix TDS 680B, 1 GS).

For the imaging studies a cooled ICCD camera (Princeton Instruments ICCD576C/1THX) with 382x574 pixel resolution was gated via a high voltage pulser (PI PG-200) using a time delay synchronized with the laser trigger signal to  $\pm 50$  ns and gate widths of 50 and 100 ns. A Nikon micro-lens was fitted to the ICCD and the focus set manually for each experiment. The pulser was linked to a PC via a detector controller (PI ST-130). Illumination was provided by a General Electric 2600 lumen fluorescent bulb using 60 Hz AC power.

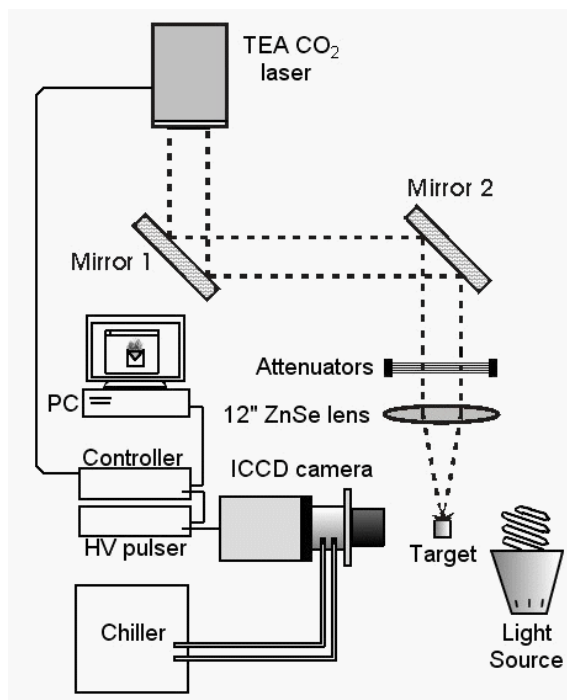


**FIGURE 1.** ICCD imaging experimental setup.

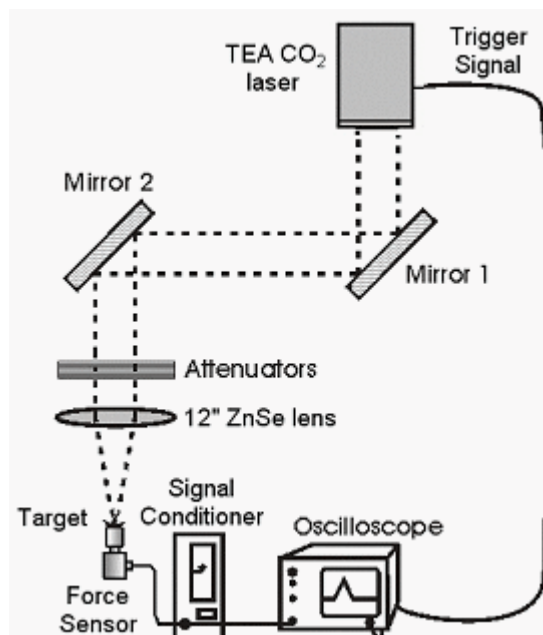


**FIGURE 2.** Force measurement experimental setup.

For the ballistics measurements, the experimental setup was virtually identical to that of the ICCD imaging experiment, except the container was placed liquid-side

down, centered atop a 9 mm circular aperture in a custom-made launch pad. The laser pulse was directed through the aperture from below via a planar gold mirror. Care was taken to keep the area downrange of the exhaust free so as to prevent any interaction between the expanding plume and the launch pad. Image sequences were taken with the ICCD camera and a standard NSTC digital video camera.

## RESULTS AND DISCUSSION

### Force Measurement

Piezoelectric force sensors were used to resolve the dominating epochs of thrust generation as force vs. time plots. Examples of typical force-time curves are shown in Figure 3 and Figure 4.

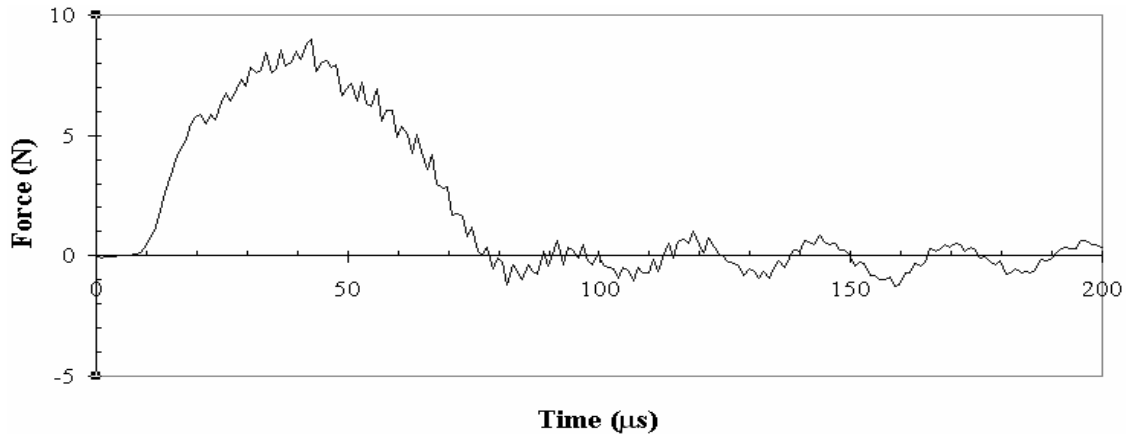


FIGURE 3. Force-time curve for water, cylindrical container, concave surface, 0.4 J,  $4 \times 10^7$  W/cm<sup>2</sup>

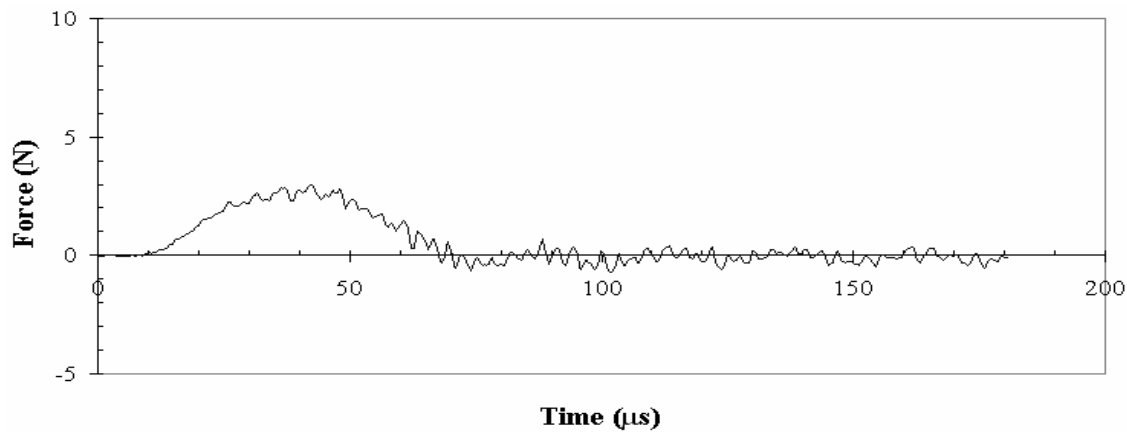


FIGURE 4. Force-time curve for hexane, cylindrical container, concave surface, 0.4 J,  $4 \times 10^7$  W/cm<sup>2</sup>

The following description generally applies to all liquids studied. An initially quiet period of about 10  $\mu\text{s}$  precedes the peaked curve observed from 10-80  $\mu\text{s}$ , which reaches its maximum value at  $\approx 40\text{-}50 \mu\text{s}$ . The smaller oscillations with period  $\approx 25 \mu\text{s}$  observed after about 100  $\mu\text{s}$  in Figure 3 and Figure 4 arise from the sensor returning to its equilibrium state via damped spring-like internal oscillations. Note that plasma events observed by ICCD imaging system were noted to occur within 1-5  $\mu\text{s}$ . The rise time of the force sensors was on the order of 5  $\mu\text{s}$ , so it was expected that any plasma-related force generation would be undetected. Derived  $C_m$  data for hexane, ethanol, and water are presented in Table 2.

**TABLE 2. Liquid Coupling Coefficients (dyne/W) (0.4 J,  $4 \times 10^7 \text{ W/cm}^2$ ).**

| Surface | Container | Hexane     | Ethanol    | Water      |
|---------|-----------|------------|------------|------------|
| Flat    | Cone      | $23 \pm 1$ | $49 \pm 6$ | $47 \pm 5$ |
|         | Cylinder  | $22 \pm 3$ | $50 \pm 3$ | $43 \pm 4$ |
| Concave | Cone      | $24 \pm 3$ | $56 \pm 3$ | $56 \pm 6$ |
|         | Cylinder  | $22 \pm 3$ | $56 \pm 4$ | $60 \pm 6$ |

Convex geometries were investigated but demonstrated uniformly poor performance compared to flat and concave geometries, and we have excluded them from direct consideration. In the case of hexane, a volume-absorbing liquid, we see virtually no change in  $C_m$  between flat and concave surfaces. Conversely, both ethanol and water - surface-absorbing liquids - experience a significant increase in  $C_m$  as the surface becomes more concave. This result is shown in Figure 5, and indicates a linear relationship with a slope of approximately 10 dyne/W per  $\text{cm}^{-1}$  of curvature (*i.e.* inverse radius).

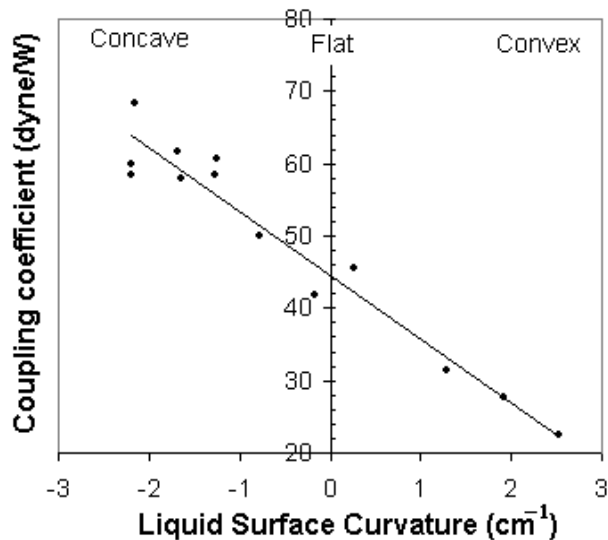


**FIGURE 5.**  $C_m$  vs. surface curvature, water, 0.4 J,  $4 \times 10^7 \text{ W/cm}^2$

## ICCD Ballistics

As mentioned, the force measurements were insensitive to plasma formation regimes, thus it was desirable to develop an independent technique in order to confirm

the results and determine if any additional impulse was imparted by plasma or splashing regimes. Ballistic trials were conducted in order to derive values of  $C_m$  from the observed momentum transfer. The target was observed to launch up to 5 cm into the air during experiments. The maximum height observed was used to derive the momentum transferred and thus  $C_m$ . The ballistics data corroborates the force measurement results, as shown in Table 3 for a constant spot size of about 3 mm<sup>2</sup>.

**TABLE 3. Liquid Coupling Coefficients (dyne/W).**

| Energy (J) | Irradiance (W/cm <sup>2</sup> ) | Force Sensor (max 10 N) | Force Sensor (max 500 N) | Ballistics |
|------------|---------------------------------|-------------------------|--------------------------|------------|
| 0.4        | $4 \times 10^7$                 | $110 \pm 14$            | -                        | $98 \pm 9$ |
| 1.2        | $1 \times 10^8$                 | $22 \pm 3$              | $53 \pm 21$              | $37 \pm 5$ |
| 3.6        | $5 \times 10^8$                 | -                       | $14 \pm 3$               | $14 \pm 2$ |

This reasonable agreement in the data implies that the impulse deduced using the force sensors is the same as that measured by ballistics method; *i.e.*, that the momentum transfer observed with the force sensors is equivalent to the total impulse imparted. Therefore no additional momentum transfer occurs as a product of plasma formation or splashing, and thus we may assume that the observed force curves are indicative of the force generation process as a whole.

### ICCD Imaging

Time-resolved ICCD images were taken to document the various regimes of ablation. These images were compared with the force data to gain an understanding of the processes important for force generation. Two distinct behaviors could be distinguished in comparing surface-absorbing and volume-absorbing liquids, as shown in Figure 6 for the four liquids studied.

In volume-absorbing liquids, the major observable process is volume boiling. Hexane was found to boil at all observed irradiances. At lower irradiances ( $10^6$  to  $10^7$  W/cm<sup>2</sup>), no vapor plume was observed, but increasing the irradiance to about  $10^8$  W/cm<sup>2</sup> resulted in plasma initiation, significant vapor plume formation, and boiling behavior.

**TABLE 4. Mass Removal by Liquid (mg) (0.4 J,  $4 \times 10^7$  W/cm<sup>2</sup>)**

| Timescale     | Hexane    | Ethanol    | Isopropanol | Water      |
|---------------|-----------|------------|-------------|------------|
| 0-100 $\mu$ s | 0         | $2 \pm 1$  | $1 \pm 1$   | $1 \pm 1$  |
| total process | $4 \pm 1$ | $51 \pm 6$ | $51 \pm 2$  | $51 \pm 5$ |

Surface-absorbing liquids are typified by the growth of a plume of ablated material, accompanied by the formation of a roughly hemispherical depression or cavity at the liquid surface. This behavior is demonstrated in Figure 6 by ethanol, isopropanol, and water. Vaporization can be seen in the form of an ablated plume of material above the liquid surface. In the present study, this plume formation occurs for approximately 100  $\mu$ s after the arrival of laser pulse. A significant force on the order of 5-10 N was detected using the piezoelectric sensors during this same time period. The vaporization plume typically reaches a maximum height of about 1.5 cm before dissipating and being overtaken by splashing at 100-200  $\mu$ s after the laser pulse.

Splashing accounted for the majority of the observed mass removal during the entire process, greater than 95% as shown in Table 4.

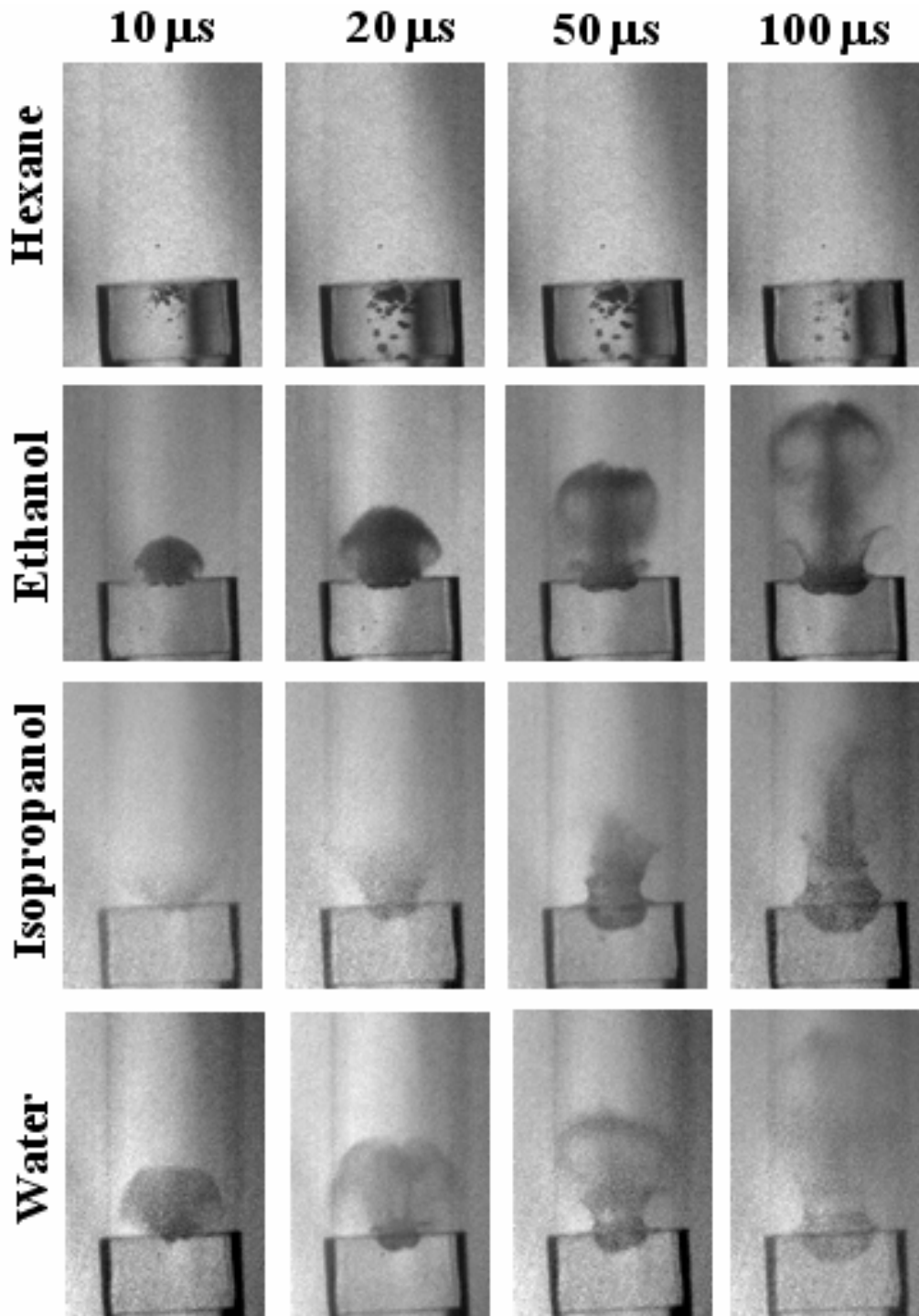


**FIGURE 6.** ICCD images of ablated liquids.

No additional momentum transfer was detected by force measurement during the time period when splashing was observed; thus, splashing is a pure mass-loss process, the minimization of which is desirable.

Observation of the growth rates of the vapor plume fronts led to the results for initial velocities presented in Table 5. Surface-absorbing liquids in this study demonstrated transonic to supersonic expansion, whereas the expansion plume of hexane, even at higher irradiance, exhibited only subsonic to transonic expansion.

**TABLE 5. Initial Plume Front Velocities ( $0.4 \text{ J}, 4 \times 10^7 \text{ W/cm}^2$ ).**

| Liquid         | Hexane       | Ethanol      | Isopropanol  | Water        |
|----------------|--------------|--------------|--------------|--------------|
| Velocity (m/s) | unobservable | $419 \pm 13$ | $303 \pm 50$ | $838 \pm 29$ |

After correcting for distortion produced by the cylindrical container, the cavity at the liquid surface was modeled as half of an oblate spheroid for the purposes of determining mass removal rates from volume loss. The liquid upheaval around the rim of the cavity was subtracted from this value. This calculation reveals that very little of the liquid mass (less than about 5 mg) was actually lost in the first 100  $\mu\text{s}$  – in fact, most of the liquid in this initial stage is simply displaced as the cavity grows. The cavity formation at early timescales does not directly contribute to the total mass loss. The cavity formation for surface-absorbing liquids appears to proceed in two distinct stages – an initial period of rapid growth until about 100-200  $\mu\text{s}$ , and a subsequent period of slower growth after this time, as shown in Figure 7. The time at which this transition occurs is the same as that observed in ICCD imaging and force measurements, which defines the shift from vaporization to splashing.

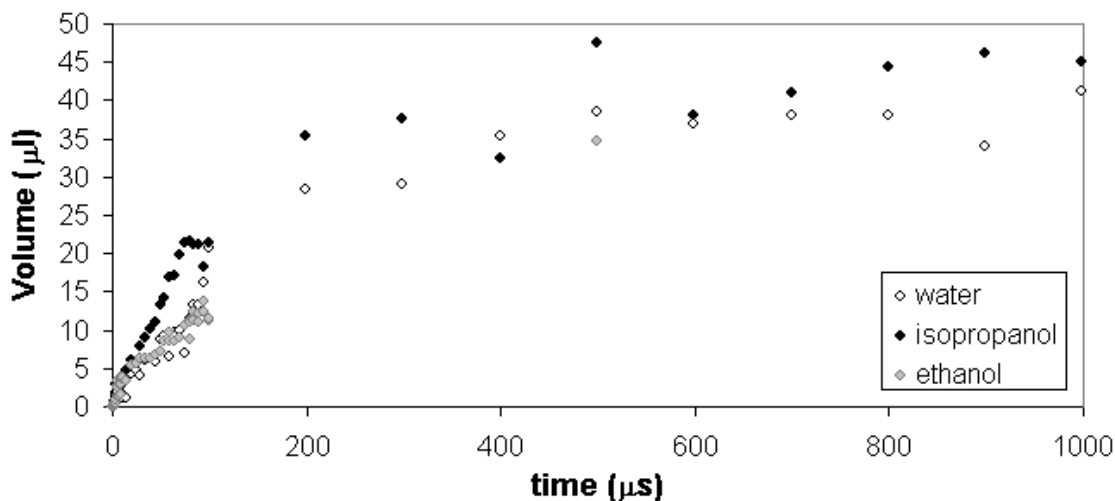


**FIGURE 7.** Cavity growth over time.

In hexane, localized boiling was observed along the column of laser propagation. Even so, there was little to no cavity formation at lower irradiances ( $10^6$ - $10^7 \text{ W/cm}^2$ ), and a calculation of cavity volume in this manner was thus unreliable.

The total mass removal was measured by weighing the liquid samples before and after the experiment. Calculated mass removal is displayed in Table 4 for flat liquid surfaces in the cylindrical container. Bulk splashing of the liquid pulls away greater

than 95% of the total mass lost. Since splashing phenomena occur at velocities 10-100 times slower than velocities typical for vaporization (500-1000 m/s), this significantly impairs the efficiency of this mode of propulsion.

The timescale for the observed cavity and plume growth above the liquid surface is the same as that for the observed force transfer, and the conclusion can certainly be drawn that most of the imparted momentum is generated by vaporization processes. The momentum transfer results in a force-time curve similar to curves of pressure vs. time presented by Kim and Grigoropoulos [3]. In light of the new evidence, we propose the following mechanism for cavity formation and force generation:

The laser pulse imparts energy to the liquid surface, which begins to vaporize. The rapidly ejected material collects above the surface, temporarily forming a high-pressure region. As the pressurized vapor in turn acts on the liquid, the surface of the liquid is pushed back to form a cavity. As a result of the pressure center interacting with the available liquid surface within the cavity, the pressure is converted to overall thrust.

The observed increase in  $C_m$  with increasing concavity is reasonable for a pressure-driven mechanism. The proposed differences are illustrated in Figure 8.

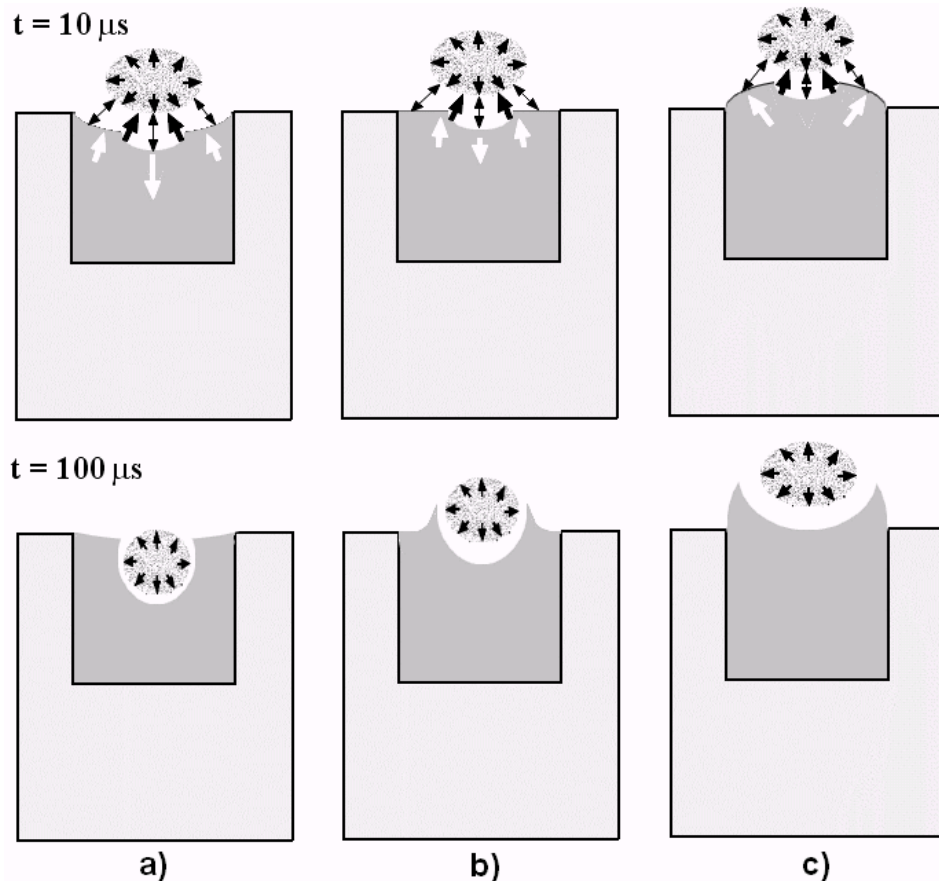


**FIGURE 8.** Qualitative presentation on variations in the geometry of the liquid surface and the evolution of pressure formation at 10 and 100  $\mu\text{s}$ , a) – concave, b) – flat and c) – convex surfaces.

Ablation from any of these surfaces will tend to direct the vaporized material into a central region, concentrating the vapor and forming a high-pressure region. For the

concave surface (Figure 8a), the liquid displaced by cavity growth is diverted to the liquid rim, so that the cavity walls rise as the cavity center descends. A similar phenomenon occurs for the flat surface, but significant radial displacement occurs in the cavity rim (Figure 8b). Consequentially, the cavity walls never attain the same height as for the concave case, and the cavity does not descend as deep into the liquid. Finally, for convex surfaces, almost all of the displaced liquid is diverted radially (Figure 8c), and as a result, the cavity walls do not experience significant growth in height. To summarize, ablation from a concave surface results in a cavity shape that surrounds the ablated vapor. Such geometry provides the highest pressure-induced thrust comparing to flat and convex cases.

Using force measurement data, comparison of the timelines for different surface concavity reveals that in each case, the force curves begin at about 5-10  $\mu\text{s}$ . However, the total time of the interaction varies from about 80  $\mu\text{s}$  for a typical concave surface up to about 120  $\mu\text{s}$  for a typical convex surface. These results suggest that the convex surfaces support longer interaction with the pressurized region, and still are exhibiting reduced coupling.

## CONCLUSIONS

The dominant mechanism of force generation in the laser ablation of liquids was studied using time-resolved piezoelectric force sensing and ICCD imaging techniques. For surface-absorbing liquids, this mechanism involves initial vaporization and the formation of a high-pressure region above the liquid. Subsequent effects include the formation of an observable cavity or depression in the surface and the growth of a significant vaporization plume. At the same laser irradiance and energy, volume-absorbing liquids exhibit boiling but no plume or cavity formation.

The vaporization regime occurs approximately during the first 100  $\mu\text{s}$  after the laser pulse arrival, resulting in a peak force at about 40-50  $\mu\text{s}$  for both surface-absorbing and volume-absorbing liquids. Splashing effects, which are responsible for greater than 95% of the total mass loss, are observed after about 100  $\mu\text{s}$  for both surface-absorbing and volume-absorbing liquids. Increasing the concavity of the liquid surface was found to alter the interaction time of the ablation process from about 80  $\mu\text{s}$  for a concave surface to about 120  $\mu\text{s}$  for a convex surface.

Increasing the concavity of the liquid surface was also found to directly increase the coupling coefficient for surface-absorbing liquids, while volume-absorbing liquids were insensitive to these changes. A corresponding but diminished sensitivity of volume-absorbing liquids to the container geometry was noted that was absent for surface-absorbing liquids. Surface-absorbing liquids demonstrated greater coupling (up to 150 dyne/W) than volume absorbers (up to 50 dyne/W) for the range of irradiances studied ( $10^6$ - $10^9$  W/cm<sup>2</sup>). This suggests that surface absorption should be preferable for any practical use of this form of propulsion.

## FUTURE WORK

The study of appropriate irradiance regimes for the laser ablation of liquids is called for, and analysis of the appropriate roll-off curves is in progress. Additionally, scaling experiments varying the container geometry and laser spot size are underway to determine any relationship to the coupling coefficient.

A major challenge to any implementation of liquid propellants is the amount of mass loss that occurs during the ablation process. Vaporization accounts for less than 5% of this total mass loss, which has been observed to proceed mainly as a result of liquid splashing at later time periods, as shown in Table 4. If the splashing could be reduced or eliminated – for instance by incorporating a gel or melting solid element like water ice as a propellant source, the process would be significantly improved, especially as concerns any potential use for propulsion. Experimental testing has been started on several materials including ice.

## ACKNOWLEDGMENTS

This work would not have been possible without financial support by ERC, Inc., The Air Force Propulsion Directorate, and The University of Alabama in Huntsville. Thanks to all members of the Laser Propulsion Group at UAH for providing helpful support and suggestions. Special thanks also go to Gene Nelson of UAH for fashioning the quartz containers used in these experiments.

## REFERENCES

1. T. Yabe, R. Nakagawa, M. Yamaguchi, T. Ohkubo, K. Aoki, C. Baasandash, H. Oozono, T. Oku, K. Taniguchi, M. Nakagawa, M. Sakata, Y. Ogata, and G. Inoue, "Simulation and Experiments on Laser Propulsion by Water Cannon Target" in *First International Symposium on Beamed Energy Propulsion-2002*, edited by Andrew V. Pakhomov, AIP Conference Proceedings 664, American Institute of Physics, Huntsville, AL, 2003, pp. 185-193.
2. T. Ohkubo, T. Yabe, S. Miyazaki, C. Baasandash, K. Taniguchi, A. Mabuchi, D. Tomita, Y. Ogata, J. Hasegawa, and K. Horioka, "Laser Propulsion Using Metal-Free Water Cannon Target" in *Beamed Energy Propulsion-2004*, edited by Andrew V. Pakhomov and Leik N. Myrabo, AIP Conference Proceedings 766, American Institute of Physics, Troy, New York, 2005, pp. 394-405.
3. D. Kim and C. P. Grigoropoulos, *Applied Surface Science*, **127-129**, 53-58 (1998).
4. E. Sterling, A. V. Pakhomov, C. W. Larson and F B. Mead, Jr., "Absorption-Enhanced Liquid Ablatants for Propulsion with TEA CO<sub>2</sub> Laser" in *Beamed Energy Propulsion-2004*, edited by Andrew V. Pakhomov and Leik N. Myrabo, AIP Conference Proceedings 766, American Institute of Physics, Troy, New York, 2005, pp. 474-481.
5. E. Sterling. "Absorption-Enhanced Liquid Ablatants for Laser Propulsion with TEA CO<sub>2</sub> Laser", M.S. Thesis, The University of Alabama in Huntsville, 2005.
6. Coblenz Society, Inc., "Evaluated Infrared Reference Spectra" in **NIST Chemistry WebBook, NIST Standard Reference Database Number 69**, Eds. P.J. Linstrom and W.G. Mallard, June 2005, National Institute of Standards and Technology, Gaithersburg MD, 20899 (<http://webbook.nist.gov>).
7. D. J. Segelstein. "The Complex Refractive Index of Water". M.S. Thesis, The University of Missouri-Kansas City, 1981.